

Source Localization Using Recursively Applied and Projected (RAP) MUSIC

John C. Mosher and Richard M. Leahy

Abstract—A new method for source localization is described that is based on a modification of the well-known MUSIC algorithm. In classical MUSIC, the array manifold vector is projected onto an estimate of the signal subspace. Errors in the estimate of the signal subspace can make localization of multiple sources difficult. Recursively applied and projected (RAP) MUSIC uses each successively located source to form an intermediate array gain matrix and projects both the array manifold and the signal subspace estimate into its orthogonal complement. The MUSIC projection to find the next source is then performed in this reduced subspace. Special assumptions about the array manifold structure, such as Vandermonde or shift invariance, are not required. Using the metric of principal angles, we describe a general form of the RAP-MUSIC algorithm for the case of diversely polarized sources. Through a uniform linear array simulation with two highly correlated sources, we demonstrate the improved Monte Carlo error performance of RAP-MUSIC relative to MUSIC and two other sequential subspace methods: S and IES-MUSIC. We then demonstrate the more general utility of this algorithm for multidimensional array manifolds in a magnetoencephalography (MEG) source localization simulation.

Index Terms—Array signal processing, EEG, MEG, MUSIC, signal subspace, source localization.

I. INTRODUCTION

SIGNAL subspace methods in array processing encompass a range of techniques for localizing multiple sources by exploiting the eigenstructure of the measured data matrix. Multiple signal classification (MUSIC) [1], [2] and its many variants are among the more frequently studied subspace methods [3]. The attractions of these MUSIC methods are twofold. First, they can provide computational advantages over direct least squares methods in which all sources are located simultaneously. More importantly, they also allow exhaustive searches over the parameter space for each source, thereby avoiding potential problems with local minima encountered in searching for multiple sources over a nonconvex error surface. Subspace methods have been most widely studied in application to the problem of direction of arrival estimation for narrowband linear equally spaced arrays. Other applications involve broadband and near-field sources and arrays with arbitrary element locations. In these cases, range and azimuth may become additional parameters over which the search must

be conducted. The problem can become even more involved when the sources are diversely polarized, such that the array manifolds required to model the sources with unknown polarization become multidimensional. Subspace methods can also be applied to nontraditional array processing problems, for example, the localization of quasistatic electromagnetic sources from electrophysiological and meteorological data [4], [5].

One important application of subspace methods is to the localization of equivalent current dipoles in the human brain from measurements of scalp potentials or electroencephalogram (EEG) and external magnetic fields or magnetoencephalogram (MEG) (collectively E/MEG) [6]. These current dipoles represent the foci of neural current sources in the cerebral cortex associated with neural activity in response to sensory, motor, or cognitive stimuli. In this case, the current dipoles have three unknown location parameters and an unknown dipole orientation (which is modeled in a similar way to the polarization vector in the diversely polarized source problem treated in [1], [2], and [7]). A direct search for the location and orientation of multiple sources involves solving a highly nonconvex optimization problem. Problems with convergence to local minima have motivated other E/MEG researchers to resort to search strategies such as simulated annealing and the use of genetic algorithms. As an alternative approach, we investigated a signal subspace approach based on the MUSIC algorithm [4], [8]. However, two problems often arise in practice. First, errors in estimating the signal subspace can make it difficult to differentiate “true” from “false” peaks in the MUSIC metric. Second, automatically finding several local maxima in the MUSIC metric becomes difficult as the dimension of the source space increases.

Recursively applied and projected (RAP)-MUSIC overcomes these problems by using a recursive procedure in which each source is found as the global maximizer of a different cost function. In essence, the method works by applying a MUSIC search to a modified problem in which we first project both the estimated signal subspace and the array manifold vector away from the subspace spanned by the sources that have already been found. We describe the RAP-MUSIC method using *principal angles* [9], which provide a framework for comparing signal subspaces and have previously been used in other related subspace signal processing problems [2], [10], [11], [12]. Since we are primarily interested in the E/MEG source localization problem, we have restricted our attention to methods that do not impose specific constraints on the

Manuscript received May 27, 1997; revised July 20, 1998. The associate editor coordinating the review of this paper and approving it for publication was Prof. Chi Chung Ko.

J. C. Mosher is with the Los Alamos National Laboratory, Los Alamos, NM 87545 USA.

R. M. Leahy is with the Signal and Image Processing Institute, University of Southern California, Los Angeles, CA 90089-2564 USA.

Publisher Item Identifier S 1053-587X(99)00759-X.

form of the array manifold. For this reason, we do not consider methods such as ESPRIT [13] or ROOT-MUSIC [3], which exploit shift invariance or Vandermonde structure in specialized arrays.

In Sections II and III, we briefly review the problem formulation, and for comparative purposes, we describe classical MUSIC in terms of principal angles. We then develop RAP-MUSIC in Section IV for the general case of “diversely polarized” sources [1], [2], [7]. A comparison of this method, both in terms of formulation using principal angles and Monte Carlo performance evaluation, is presented for three alternative sequential algorithms: S-MUSIC [14], IES-MUSIC [15] and R-MUSIC [16]. We then present an MEG example to highlight diversely polarized applications. A preliminary version of this work was presented in [17].

II. BACKGROUND

We consider the problem of estimating the parameters of r sources impinging on an m -sensor element array. Each source is represented by an $m > r$ (possibly complex) array manifold vector $\mathbf{a}(\theta)$. Each source parameter θ may be multidimensional, and the collection of the r manifold parameters is designated $\Theta = \{\theta_1, \dots, \theta_r\}$. The manifold vectors collectively form an $m \times r$ array transfer matrix

$$\mathbf{A}(\Theta) = [\mathbf{a}(\theta_1), \dots, \mathbf{a}(\theta_r)] \quad (1)$$

which we assume to be of full column rank r for any set of r distinct source parameters Θ , i.e., no array ambiguities exist. Associated with each array manifold vector is a time series $s(t)$, and the data are acquired as $\mathbf{x}(t) = \mathbf{A}(\theta)\mathbf{s}(t) + \mathbf{n}(t)$, where $\mathbf{s}(t)$ is the vector of r time series at time t . The additive noise vector $\mathbf{n}(t)$ is assumed to be zero mean with covariance $E\{\mathbf{n}(t)\mathbf{n}^H(t)\} = \sigma_n^2\mathbf{I}$, where superscript “ H ” denotes the Hermitian transpose.

The autocorrelation of $\mathbf{x}(t)$ can be partitioned as

$$\begin{aligned} \mathbf{R} &= E\{\mathbf{x}(t)\mathbf{x}^H(t)\} \\ &= \mathbf{A}(\Theta)(E\{\mathbf{s}(t)\mathbf{s}^H(t)\})\mathbf{A}(\Theta)^H + \sigma_n^2\mathbf{I} \\ &= \Phi[\Lambda + \sigma_n^2\mathbf{I}]\Phi^H = \Phi_s\Lambda_s\Phi_s^H + \Phi_n\Lambda_n\Phi_n^H \end{aligned} \quad (2)$$

where we have assumed that the time series are uncorrelated with the noise. We assume that the correlation of the signal time series yields a full rank matrix $\mathbf{P} = E\{s(t)s^H(t)\}$, and $\mathbf{A}(\Theta)\mathbf{P}\mathbf{A}(\Theta)^H$ can be eigendecomposed as $\Phi_s\Lambda\Phi_s^H$, where Φ_s contains the r eigenvectors corresponding to the nonzero eigenvalues, and $\text{span}(\mathbf{A}(\Theta)) = \text{span}(\Phi_s)$. The r eigenvalues of this decomposition combine with the noise covariance to form $\Lambda_s = \Lambda + \sigma_n^2\mathbf{I}$ with the eigenvalues in the diagonal Λ_s arranged in decreasing order. The diagonal Λ_n comprises the $m - r$ repeated eigenvalues σ_n^2 , and Φ_n contains the corresponding $m - r$ eigenvectors. Thus, (2) represents the well-known partitioning of the covariance matrix into *signal subspace* ($\text{span}(\Phi_s)$) and *noise-only subspace* ($\text{span}(\Phi_n)$) terms.

Let $\hat{\mathbf{R}}$ denote the sample covariance. We designate the first r eigenvectors of $\hat{\mathbf{R}}$ as $\hat{\Phi}_s$, i.e., a set of vectors that span our estimate of the signal subspace; similarly, we designate

the estimated noise-only subspace $\hat{\Phi}_n$ using the remaining eigenvectors.

Finally, we generalize the array manifold vector for the case of vector sources representing, for instance, diverse polarization [1], [2], [7], in conventional array processing or current dipoles in EEG and MEG source localization [8]. In this case, the array manifold vector is the product of a multidimensional array manifold or gain matrix and a polarization or orientation vector

$$\mathbf{a}(\theta) = \mathbf{G}(\rho)\phi \quad (3)$$

and we may view the parameter set for each source as $\theta = \{\rho, \phi\}$, comprising quasilinear orientation parameters ϕ and nonlinear location parameters ρ .

III. MUSIC AND PRINCIPAL ANGLES

The MUSIC algorithm [1], [2] finds the source locations as those for which the corresponding array manifold vector is nearly orthogonal to the noise-only subspace or, equivalently, projects almost entirely into the estimated signal subspace. For the diversely polarized case, the problem becomes more complex since the signal or noise-only subspaces must be compared with the entire span of the gain matrix $\mathbf{G}(\rho)$. A natural way to compare these two subspaces is through use of *principal angles* [9] or *canonical correlations* (i.e., the cosines of the principal angles) (cf., [11]).

Let q denote the minimum of the ranks of two matrices \mathbf{A} and \mathbf{B} . The canonical or subspace correlation is a vector containing the cosines of the q principal angles that reflect the similarity between the subspaces spanned by the columns of the two matrices. The elements of the subspace correlation vector are ranked in decreasing order, and we denote the largest subspace correlation (i.e., the cosine of the smallest principal angle) as

$$\text{subcorr}(\mathbf{A}, \mathbf{B})_1. \quad (4)$$

If $\text{subcorr}(\mathbf{A}, \mathbf{B})_1 = 1$, then the two subspaces have at least a one-dimensional (1-D) subspace in common. Conversely, if $\text{subcorr}(\mathbf{A}, \mathbf{B})_1 = 0$, then the two subspaces are orthogonal. These subspace correlations are readily computed using SVD’s as described in [9].

The MUSIC algorithm finds the source locations as those for which the principal angle between the array manifold vector and the noise-only subspace is maximum. Equivalently, the sources are chosen as those that minimize the noise-only subspace correlation $\text{subcorr}(\mathbf{a}(\theta), \hat{\Phi}_n)_1$ or maximize the signal subspace correlation $\text{subcorr}(\mathbf{a}(\theta), \hat{\Phi}_s)_1$. Since the first argument is a vector and the second is already orthogonalized, the square of this signal subspace correlation is easily shown to be

$$\text{subcorr}(\mathbf{a}(\theta), \hat{\Phi}_s)_1^2 = \frac{(\mathbf{a}(\theta)^H \hat{\Phi}_s \hat{\Phi}_s^H \mathbf{a}(\theta))}{(\mathbf{a}(\theta)^H \mathbf{a}(\theta))} \quad (5)$$

where the right-hand side is the standard metric used in MUSIC [1], [2].

Principal angles can also be used to represent the MUSIC metric for multidimensional array manifolds represented by

$\mathbf{G}(\rho)$ in (3). In this case, the algorithm must compare the entire space spanned by $\mathbf{G}(\rho)$ with the signal subspace. A linear combination of the columns of $\mathbf{G}(\rho)$ that lies entirely in the signal subspace yields $subcorr(\mathbf{G}(\rho), \hat{\Phi}_s)_1 = 1$, which indicates the presence of a source with nonlinear parameters ρ . It is again straightforward to equate the subspace correlation with Schmidt's metric for diversely polarized MUSIC:

$$subcorr(\mathbf{G}(\rho), \hat{\Phi}_s)_1^2 = \lambda_{\max}(\mathbf{U}_G^H \hat{\Phi}_s \hat{\Phi}_s^H \mathbf{U}_G) \quad (6)$$

where \mathbf{U}_G contains the left singular vectors of $\mathbf{G}(\rho)$, and $\lambda_{\max}(\cdot)$ is the maximum eigenvalue of the enclosed expression.

The nonlinear source locations ρ can be found as those for which (6) is approximately unity. The direction of polarization (in the diversely polarized case) or the dipole orientation (in MEG and EEG) is then found as the normalized quasilinear parameter vector ϕ that must be multiplied by $\mathbf{G}(\rho)$ to produce the array manifold vector $\mathbf{a}(\theta)$ that lies in the span of $(\hat{\Phi}_s)$. The quasilinear parameters can be derived from the eigenvector corresponding to the maximum eigenvalue in (6). Equivalently, the singular vectors from the SVD's performed to compute $subcorr(\cdot)$ can be used to form ϕ [9], [16].

IV. RAP-MUSIC

If the r -dimensional signal subspace is estimated perfectly, then the sources are simply found as the r global maximizers of (6). Errors in our estimate $\hat{\Phi}_s$ reduce (6) to a function with a single global maximum and at least $(r-1)$ local maxima. Finding the first source is simple: Over a sufficiently densely sampled grid of the nonlinear parameter space ρ , find the global maximum of

$$\hat{\rho}_1 = \arg \max_{\rho} (subcorr(\mathbf{G}(\rho), \hat{\Phi}_s)_1). \quad (7)$$

We then extract the corresponding eigenvector in (6) to form the quasilinear parameter estimate $\hat{\phi}$. The estimate of the parameters of the first source is denoted $\hat{\theta}_1 = \{\hat{\rho}_1, \hat{\phi}_1\}$, and the first estimated array manifold vector is formed as

$$\mathbf{a}(\hat{\theta}_1) = \mathbf{G}(\hat{\rho}_1) \hat{\phi}_1. \quad (8)$$

Identifying the remaining local maxima becomes more difficult since nonlinear search techniques may miss shallow or adjacent peaks and return to a previous peak. We also need to locate the r best peaks rather than any r local maxima. Numerous techniques have been proposed in the past to enhance the "peak-like" nature of the spectrum (cf. [3], [10]) so that identifying these peaks becomes simpler. In highly correlated or closely spaced sources, the peaks become almost indeterminate, as shown in Fig. 1. These "peak-picking" algorithms rapidly become complex and subjective as the number of sources and the dimensionality of ρ increase.

The novelty of RAP-MUSIC is to avoid this peak-picking problem entirely. We instead remove the component of the signal subspace that is spanned by the first source and then perform a search to find the second source as the global maximizer over this modified subspace. In this way, we replace the problem of finding r local maxima with one in which

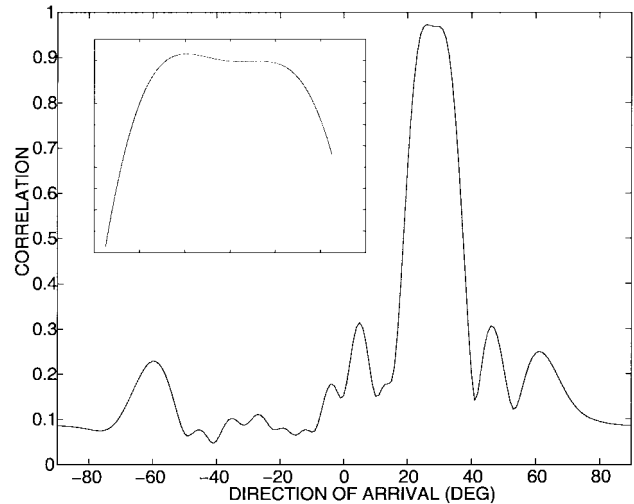


Fig. 1. Two sources arrive from 25 and 30° at a uniform linear array. The MUSIC metric (5) is plotted as a function of the angle of arrival. The two peaks are not readily discernible, as shown in the inset enlargement. An algorithm must be trained to "peak-pick" the second source, shown here at 30°. Such algorithms must also distinguish between the two "true" peaks and all other "local" peaks, as illustrated in this figure. The projected forms of MUSIC presented in this paper make detection of the second peak more obvious as well as improve statistical performance in locating the sources.

we find the sources as r global maxima over their respective modified signal subspaces.

The method can be viewed simply in terms of the subspace correlation functions described above. Define the orthogonal projector for $\mathbf{a}(\hat{\theta}_1)$ as

$$\Pi_{\mathbf{a}(\hat{\theta}_1)}^\perp = \mathbf{I} - (\mathbf{a}(\hat{\theta}_1) \mathbf{a}^H(\hat{\theta}_1)) / (\mathbf{a}^H(\hat{\theta}_1) \mathbf{a}(\hat{\theta}_1)) \quad (9)$$

and apply this operator to both arguments of the $subcorr(\cdot)$ function. The second source is then found as the global maximizer

$$\hat{\rho}_2 = \arg \max_{\rho} (subcorr(\Pi_{\mathbf{a}(\hat{\theta}_1)}^\perp \mathbf{G}(\rho), \Pi_{\mathbf{a}(\hat{\theta}_1)}^\perp \hat{\Phi}_s)_1). \quad (10)$$

Here, we have projected both our signal subspace estimate and the multidimensional array manifold away from the first solution and then found the maximum subspace correlation (minimum principal angle) between these two projected spaces. After the maximization, the quasilinear parameters are again easily extracted, and the second array manifold vector is estimated as $\mathbf{a}(\hat{\theta}_2) = \mathbf{G}(\hat{\rho}_2) \hat{\phi}_2$. We then form the orthogonal projection operator for the combination of the first two sources and proceed recursively.

By extension, the k th recursion $k = 1, \dots, r$ of RAP-MUSIC is

$$\hat{\rho}_k = \arg \max_{\rho} (subcorr(\Pi_{\hat{\mathbf{A}}_{k-1}}^\perp \mathbf{G}(\rho), \Pi_{\hat{\mathbf{A}}_{k-1}}^\perp \hat{\Phi}_s)_1) \quad (11)$$

where we define

$$\hat{\mathbf{A}}_{k-1} \equiv [\mathbf{a}(\hat{\theta}_1) \cdots \mathbf{a}(\hat{\theta}_{k-1})] \quad (12)$$

as formed from the array manifold estimates of the previous $k-1$ recursions, and

$$\Pi_{\hat{\mathbf{A}}_{k-1}}^\perp \equiv (\mathbf{I} - \hat{\mathbf{A}}_{k-1} (\hat{\mathbf{A}}_{k-1}^H \hat{\mathbf{A}}_{k-1})^{-1} \hat{\mathbf{A}}_{k-1}^H) \quad (13)$$

is the projector onto the left null space of $\hat{\mathbf{A}}_{k-1}$. The recursions are stopped once the maximum of the subspace correlation in (11) drops below a minimum threshold.

Practical considerations in low-rank E/MEG source localization lead us to prefer the use of the signal rather than the noise-only subspace [17]. The development above in terms of the signal subspace is readily modified to computations in terms of the noise-only subspace. Our experience in low-rank forms of MUSIC processing is that the determination of the signal subspace rank need not be precise, as long as the user conservatively overestimates the rank. The additional basis vectors erroneously ascribed to the signal subspace can be considered to be randomly drawn from the noise-only subspace [11]. As we described above, RAP MUSIC removes from the signal subspace the subspace associated with each source once it is found. Thus, once the true rank has been exceeded, the subspace correlation between the array manifold and the remaining signal subspace should drop markedly, and thus, additional fictitious sources will not be found.

V. OTHER SEQUENTIAL FORMS OF MUSIC

We now compare RAP-MUSIC with three other sequential forms: R-MUSIC [16], S-MUSIC [14] and IES-MUSIC [15]. All of the methods used in our comparison find the first source in the same way, i.e., as the global maximizer of $subcorr(\mathbf{a}(\theta), \hat{\Phi}_s)_1$. The manner in which the subsequent sources are found differs for each method.

A. R-MUSIC

In [16], we introduced a preliminary version of RAP-MUSIC that we refer to as R-MUSIC. The algorithm differs from RAP-MUSIC in the manner in which the sources that have already been found are used to alter the search for the next. In contrast to (11), the k th recursion $k = 1, \dots, r$ of R-MUSIC is

$$\hat{\rho}_k = \arg \max_{\rho} subcorr([\hat{\mathbf{A}}_{k-1} \mathbf{G}(\rho)], \hat{\Phi}_s)_k \quad (14)$$

where $subcorr([\hat{\mathbf{A}}_{k-1} \mathbf{G}(\rho)], \hat{\Phi}_s)_k$ denotes the k th element of the subspace correlation (i.e., the cosine of the k th ordered principal angle) between the estimated signal subspace and the concatenation of $\hat{\mathbf{A}}_{k-1}$, which are the array manifold vectors for sources already found, and $\mathbf{G}(\rho)$, which is the array gain matrix. The basis for this method is as follows. The $k-1$ sources already found produce a matrix $\hat{\mathbf{A}}_{k-1}$ whose column space is (approximately) contained in $\text{span}(\hat{\Phi}_s)$ and, hence, will yield $k-1$ principal angles (approximately) equal to zero. Once the true parameter ρ is found in $\mathbf{G}(\rho)$, then the matrix $[\hat{\mathbf{A}}_{k-1} \mathbf{G}(\rho)]$ should yield k principal angles approximately equal to zero. Equivalently, the k th ordered subspace correlation in (14) should be close to unity.

B. S- and IES-MUSIC

We now simplify the presentation to the case of two nonpolarized sources that is treated in [14] and [15]. In S-MUSIC [14], we apply the projection operator (9) to the array

manifold, but not the signal subspace, and find the second source as $\arg \max_{\theta} g(\theta)$, where

$$g(\theta) = \frac{(\mathbf{a}^H(\theta) \Pi_{\mathbf{a}(\hat{\theta}_1)}^{\perp} \hat{\Phi}_s \hat{\Phi}_s^H \Pi_{\mathbf{a}(\hat{\theta}_1)}^{\perp} \mathbf{a}(\theta))}{\|\Pi_{\mathbf{a}(\hat{\theta}_1)}^{\perp} \mathbf{a}(\theta)\|^2}. \quad (15)$$

In IES-MUSIC [15], the denominator of (15) is dropped, and the modification used is

$$g(\theta, \hat{\rho}) = \mathbf{a}^H(\theta) (\mathbf{I} - \hat{\rho}^* \Pi_{\mathbf{a}(\hat{\theta}_1)}) \hat{\Phi}_s \hat{\Phi}_s^H (\mathbf{I} - \hat{\rho} \Pi_{\mathbf{a}(\hat{\theta}_1)}) \mathbf{a}(\theta) \quad (16)$$

where $\Pi_{\mathbf{a}(\hat{\theta}_1)} = \mathbf{I} - \Pi_{\mathbf{a}(\hat{\theta}_1)}^{\perp}$. This measure is equivalent to S-MUSIC for $\hat{\rho} = 1$ and MUSIC for $\hat{\rho} = 0$. In [15], an optimal complex scalar ρ is derived for the case of two sources, which minimizes the theoretical asymptotic error variance of the second source. However, this scalar requires knowledge of the two sources θ_1 and θ_2 . Since these parameters are unknown, IES-MUSIC first obtains the estimated locations θ_1 and θ_2 from another approach, such as MUSIC, from which it forms the estimate $\hat{\rho}$. After this step, $g(\theta, \hat{\rho})$ is maximized to find the second source.

For this nonpolarized two-source problem, these algorithms may be summarized and compared using the subspace correlation function as follows.

MUSIC:

$$\hat{\theta}_2 = \arg \max subcorr(\mathbf{a}(\theta), \hat{\Phi}_s)_1^2 \quad \hat{\theta}_2 \neq \hat{\theta}_1. \quad (17)$$

S-MUSIC:

$$\hat{\theta}_2 = \arg \max subcorr(\Pi_{\mathbf{a}(\hat{\theta}_1)}^{\perp} \mathbf{a}(\theta), \hat{\Phi}_s)_1^2. \quad (18)$$

IES-MUSIC ($\hat{\rho}$ defined in [15]):

$$\hat{\theta}_2 = \arg \max \|\mathbf{I} - \hat{\rho}^* \Pi_{\mathbf{a}(\hat{\theta}_1)} \mathbf{a}(\theta)\|^2 \cdot subcorr((\mathbf{I} - \hat{\rho}^* \Pi_{\mathbf{a}(\hat{\theta}_1)}) \mathbf{a}(\theta), \hat{\Phi}_s)_1^2. \quad (19)$$

R-MUSIC:

$$\hat{\theta}_2 = \arg \max subcorr([\mathbf{a}(\hat{\theta}_1), \mathbf{a}(\theta)], \hat{\Phi}_s)_2. \quad (20)$$

RAP-MUSIC:

$$\hat{\theta}_2 = \arg \max subcorr(\Pi_{\mathbf{a}(\hat{\theta}_1)}^{\perp} \mathbf{a}(\theta), \Pi_{\mathbf{a}(\hat{\theta}_1)}^{\perp} \hat{\Phi}_s)_1. \quad (21)$$

In (18) and (19), the first argument is a vector, and the second argument is already orthogonal. Thus, (18) and (19) are readily seen to be equivalent to (15) and (16), respectively, using, for instance, (5). When viewed in terms of the subspace correlations, we see that the clear difference between RAP-MUSIC and the other sequential forms is that the projection operator is applied to both arguments before computing the subspace correlation rather than just to the array manifold, as in the case of S- and IES-MUSIC.

VI. SIMULATIONS

We present two different simulations in order to show both the performance and the utility of RAP-MUSIC. The first simulation is a conventional two-source uniform linear array example to compare with the other sequential forms. The second simulation is a three-source multidimensional manifold example, localizing three dipoles in three-dimensional (3-D) space in an MEG application.

TABLE I

COMPARISON OF ANALYTIC STANDARD DEVIATIONS AND RMS ERROR. THE NUMBER OF TIME SAMPLES REMAINS CONSTANT AT 1000, AND THE CORRELATION BETWEEN THE TWO SOURCES IS VARIED. FOR EACH OF THE 2000 MONTE CARLO REALIZATIONS, SOURCE 1 (EITHER 25 OR 30°) WAS SELECTED AS THE SOURCE WITH THE HIGHEST MUSIC PEAK. THE THEORETICAL STANDARD DEVIATION [15] AND ROOT MEAN SQUARED (RMS) ERROR OF THE SECOND SOURCE IS TABULATED. IES-MUSIC IS SHOWN WITH ITS SCALAR SET USING BOTH TRUE AND ESTIMATED VALUES. MUSIC WAS UNRELIABLE IN LOCATING THE SECOND PEAK FOR $\gamma = 0.975$, AS ILLUSTRATED IN FIG. 1

	n	1000		1000		1000		1000		1000		1000	
		γ		0.975		0.950		0.925		0.900		0.850	
	θ_2 (deg)	25	30	25	30	25	30	25	30	25	30	25	30
	Runs	1009	991	998	1002	996	1004	1007	993	995	1005	991	1009
MUSIC (deg)	Theoretical	0.531	0.555	0.294	0.308	0.214	0.224	0.174	0.182	0.132	0.138	0.088	0.092
	RMS err	--	--	0.513	0.520	0.215	0.240	0.165	0.172	0.120	0.131	0.087	0.091
S-MUSIC	Theoretical	0.534	0.559	0.296	0.310	0.216	0.226	0.175	0.183	0.133	0.139	0.089	0.093
	RMS err	0.786	0.799	0.275	0.295	0.192	0.196	0.151	0.159	0.115	0.124	0.084	0.088
IES-MUSIC	Theoretical	0.083	0.087	0.065	0.069	0.062	0.064	0.060	0.063	0.059	0.062	0.059	0.061
	RMS err, ρ	0.444	0.478	0.078	0.084	0.063	0.066	0.063	0.067	0.063	0.064	0.063	0.065
	RMS err, $\hat{\rho}$	0.867	0.914	0.188	0.210	0.106	0.113	0.083	0.084	0.070	0.072	0.064	0.067
R-MUSIC	RMS err	0.913	0.924	0.391	0.418	0.278	0.286	0.222	0.234	0.166	0.179	0.112	0.116
RAP-MUSIC	RMS err	0.805	0.854	0.153	0.165	0.087	0.093	0.070	0.072	0.064	0.065	0.062	0.064

A. Narrowband Uniform Linear Array Example

We follow the simulations in [15] in order to draw performance comparisons between the various sequential forms of MUSIC. The sensor array is the conventional uniform linear array of sensors spaced a half-wavelength apart. The sources are farfield narrowband and impinging on the array from scalar direction θ . The array manifold vector may therefore be specified as

$$\mathbf{a}(\theta) = [1, e^{j\pi \sin \theta}, \dots, e^{j\pi(m-1) \sin \theta}]^T \quad (22)$$

where $\theta = 0$ is broadside to the array, and $\|\mathbf{a}(\theta)\| = m$. The source time series are assumed to be complex zero-mean Gaussian sequences with covariance matrix \mathbf{P} . We assume 15 sensor elements and two sources at 25° and 30°. The source covariance matrix is specified as

$$\mathbf{P} = \begin{bmatrix} 1 & \gamma \\ \gamma^* & 1 \end{bmatrix} \quad (23)$$

where $|\gamma| \leq 1$ determines the degree of correlation between these two sources of equal power. The variance of the noise is set to unity, such that the signal to noise power ratio is also unity.

We simulate n samples of both the signal and noise, form the estimated data covariance matrix, and then extract the matrix $\hat{\Phi}_s$ comprising the two estimated signal subspace vectors. The noise variance is estimated as the mean of the noise-only subspace eigenvalues. For each realization, we find the maxima of the MUSIC measure in a region about each of the true solutions. The source with the better correlation is considered source θ_1 . The second source θ_2 is then found by maximizing the appropriate measure (17)–(21). In [15], closed-form formulae are presented for calculating the theoretical error variance of MUSIC, S-MUSIC, and IES-MUSIC.

Since IES-MUSIC is a “two-pass” algorithm, i.e., it requires an initial estimate of both source parameters, we used the RAP-MUSIC source estimates for the initial estimate in our Monte Carlo study, as the RAP-MUSIC solution was on average superior to the MUSIC and S-MUSIC estimates. We also ran as a comparison IES-MUSIC with ρ set to the optimal value found using the true source angles. For each estimator, we calculated a numerical root mean squared (RMS) error,

$$\text{RMS} = \left(\frac{1}{\text{Runs}} \sum_{i=1}^{\text{Runs}} (\hat{\theta}_2(i) - \theta_2)^2 \right)^{1/2} \quad (24)$$

where $\hat{\theta}_2(i)$ represents the estimate from the i th Monte Carlo run. In each of these 2000 runs, we determined which of the two MUSIC peaks in the regions about the true answer was greater and declared this source as $\hat{\theta}_1$. We then estimated the second source and tabulated the actual number of runs used for both $\theta_2 = 20^\circ$ or 30° , which is approximately evenly split at about 1000 Monte Carlo runs each.

In Table I, we held the number of time samples constant at $n = 1000$ and varied the degree of correlation between the two sources. For uncorrelated sources ($\gamma = 0$), all measures performed similarly, as also demonstrated in [15]. The differences in performance begin to arise as we increase the correlation to $\gamma = 0.7$, where we observe that IES-MUSIC and RAP-MUSIC have RMS error about 25% better than MUSIC and S-MUSIC and 50% better than R-MUSIC. At $\gamma = 0.925$, we see that RAP-MUSIC continues to have performance comparable with that of perfect IES-MUSIC but that estimated IES-MUSIC is beginning to degrade in comparison; MUSIC and S-MUSIC have RMS error almost twice that of IES-MUSIC and RAP-MUSIC at this correlation, and R-MUSIC has the largest RMS error.

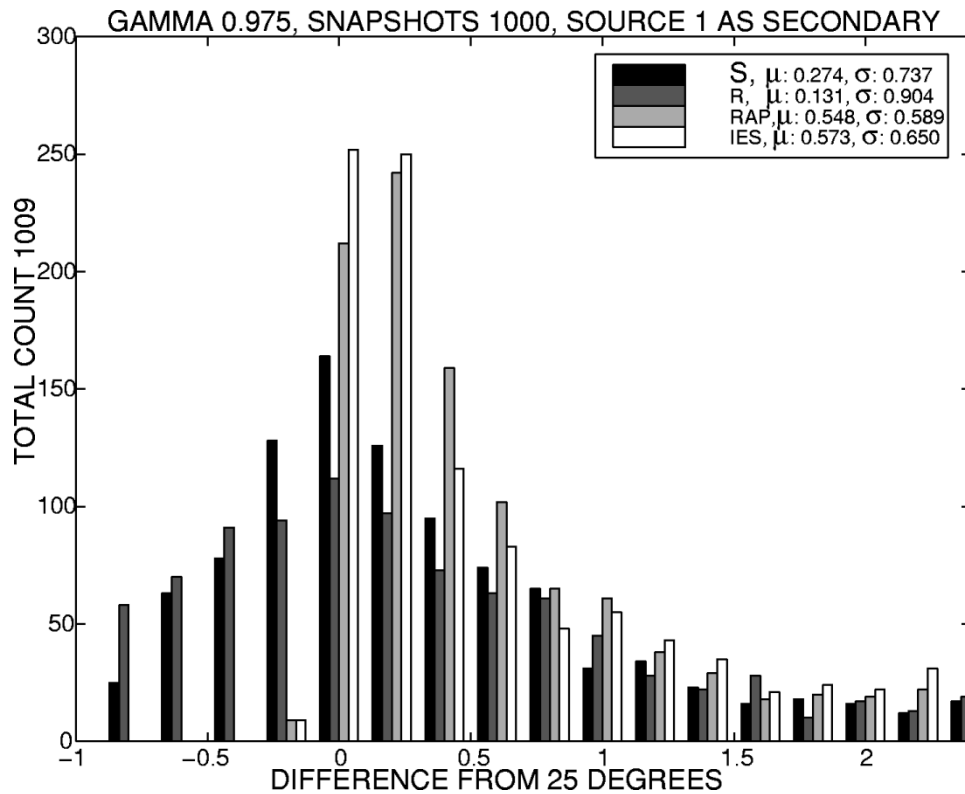


Fig. 2. From the first column of Table I, histogram of the source localization results for 1009 Monte Carlo runs, a correlation of 0.975 between the two sources at 25 and 30°, and 1000 time samples per simulation. For the source at 25°, we see that R-MUSIC has the lowest bias, whereas RAP-MUSIC and IES-MUSIC have developed a more noticeable bias toward the other source. Both RAP-MUSIC and IES-MUSIC, however, exhibit lower variance (σ in the legend) such that the RMS error of all four sequential techniques is approximately the same for this highly correlated case, as shown in Table I.

By $\gamma = 0.975$, all methods are experiencing comparable difficulty in estimating the sources and have deviated significantly from the theoretical variances. MUSIC is particularly poor at this correlation since in many trials, an adequately detectable peak did not occur in the region around the true answer, as illustrated in Fig. 1. In Fig. 2, a histogram of Monte Carlo results for this highly correlated case shows the bias and variance differences between the competing sequential techniques. Both S-MUSIC and R-MUSIC appear much less biased but have higher variance than IES-MUSIC and RAP-MUSIC, such that all techniques exhibit similar RMS performance for this highly correlated case. At a slightly lower correlation ($\gamma = 0.95$), the bias drops markedly in all techniques to 0.1° or less, such that the RMS error reflects more closely the standard deviation of each technique.

In general, the RMS error of MUSIC and S-MUSIC match the theoretical asymptotic error variances established in [15] quite well, but the theoretical calculations for IES-MUSIC tend to underestimate RMS error. IES-MUSIC performance using the optimally designed ρ agrees quite well with the theoretical values, but this performance obviously requires prior knowledge of the true solution. RAP-MUSIC consistently maintains an improved RMS error over that of IES-MUSIC, and we note again that IES-MUSIC depends on some other technique in order to arrive at an initial set of source estimates.

These RMS errors were calculated at a relatively large number of time samples. We also tested small sample performance in which we held the correlation constant at $\gamma = 0.9$ and varied

the number of time samples. As shown in Table II, at lower numbers of time samples, we generally had a difficult task determining a second MUSIC peak, and the MUSIC results were unreliable. As in Table I, RAP-MUSIC consistently maintained improved performance over the other methods.

B. MEG Simulation

We now illustrate the ability of RAP-MUSIC to extract multiple current dipole sources in the brain from MEG data. See [8] and [16] for more details of the formulation and [6] for an introduction to this problem. Compared with the narrowband simulation above, the MEG source localization problem has several additional difficulties. Each dipolar source has a 3-D location parameter and an additional 3-D quasi-linear parameter for the orientation of the source. The underlying physics of quasi-static electromagnetics yields an array manifold that may exhibit partial array ambiguities for multiple sources, complicating the 3-D peak search. The sources of interest usually have transient time courses that limit the number of time samples that can be used for localization.

In this simulation, we make the simplifying assumption that the brain is a spherical homogenous conductor so that closed-form expressions are available for the external magnetic fields produced by the current dipoles. We arrange 229 radially oriented sensors about 2 cm apart on the upper hemisphere of a 12 cm virtual sphere. Each sensor is modeled as a first-order gradiometer with a baseline separation of 5 cm. For exemplary purposes, we arrange three sources in the same z -plane: $z = 7$

TABLE II
 NUMBER OF TIME SAMPLES IS NOW VARIED, WHEREAS THE CORRELATION BETWEEN THE TWO SOURCES IS HELD CONSTANT AT 0.9.
 AS IN TABLE I, FOR EACH OF THE 2000 MONTE CARLO REALIZATIONS, SOURCE 1 (EITHER 25 OR 30°) WAS SELECTED AS
 THE SOURCE WITH THE HIGHEST MUSIC PEAK. MUSIC WAS UNRELIABLE IN LOCATING THE SECOND PEAK FOR $n = 100$

	n	100		200		400		800	
	γ	0.9		0.9		0.9		0.9	
	θ_2 (deg)	25	30	25	30	25	30	25	30
	Runs	999	1001	1009	991	1007	993	971	1029
Music (deg)	Theoretical	0.550	0.575	0.389	0.407	0.275	0.288	0.194	0.203
	RMS err	--	--	1.161	1.115	0.386	0.467	0.187	0.204
S-MUSIC	Theoretical	0.554	0.579	0.391	0.410	0.277	0.290	0.196	0.205
	RMS err	0.823	0.887	0.458	0.489	0.263	0.295	0.166	0.181
IES-MUSIC	Theoretical	0.190	0.199	0.134	0.141	0.095	0.100	0.067	0.070
	RMS err, ρ	0.390	0.410	0.158	0.164	0.096	0.095	0.067	0.075
	RMS err, $\hat{\rho}$	0.976	1.014	0.476	0.491	0.187	0.217	0.092	0.107
R-MUSIC	RMS err	0.967	1.045	0.593	0.638	0.374	0.410	0.245	0.264
RAP-MUSIC	RMS err	0.795	0.837	0.348	0.348	0.142	0.161	0.079	0.088

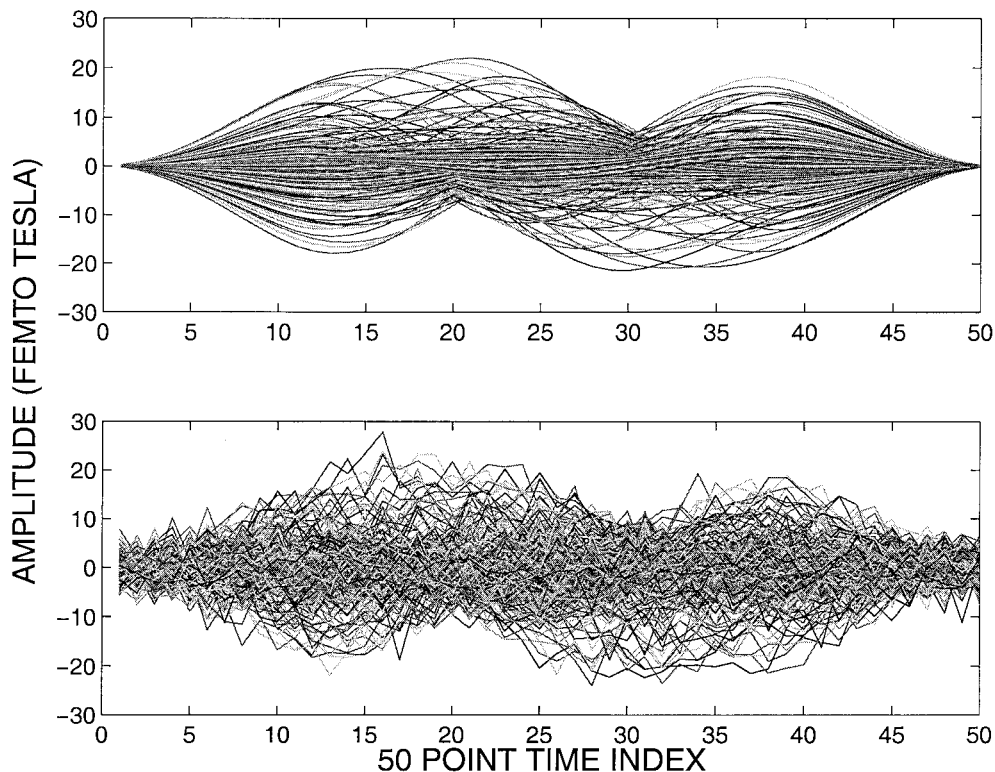


Fig. 3. Simulated MEG data for 229 sensors by 50 time snapshots. True sources are three asynchronous fixed dipoles. Gaussian white noise was added such that the squared Frobenius norm of the noiseless data matrix was 3.16 times that of the noise-only matrix, i.e., 10 dB SNR. The signal subspace was overspecified to be rank 5.

cm. We fix the orientation of each source and assign each an independent time series. We then add white Gaussian i.i.d. noise on each sensor channel. The noiseless and noisy data are displayed in Fig. 3.

An SVD of the noisy spatio-temporal data matrix clearly showed the signal subspace to be rank three; however, to illustrate insensitivity to rank overselection, we chose a signal

subspace of rank five. We created a 1.5-mm-spaced grid in the correct z -plane and computed the 3-D gain matrix $\mathbf{G}(\rho)$ for each location on the grid. We then computed the standard MUSIC metric (5) between each gain matrix and the rank five signal subspace. The result is shown in Fig. 4 as the image $1/(1 - s_1^2)$, where s_1 is the value of $\text{subcorr}(\mathbf{G}(\rho), \hat{\Phi}_s)_1$ at each grid point.

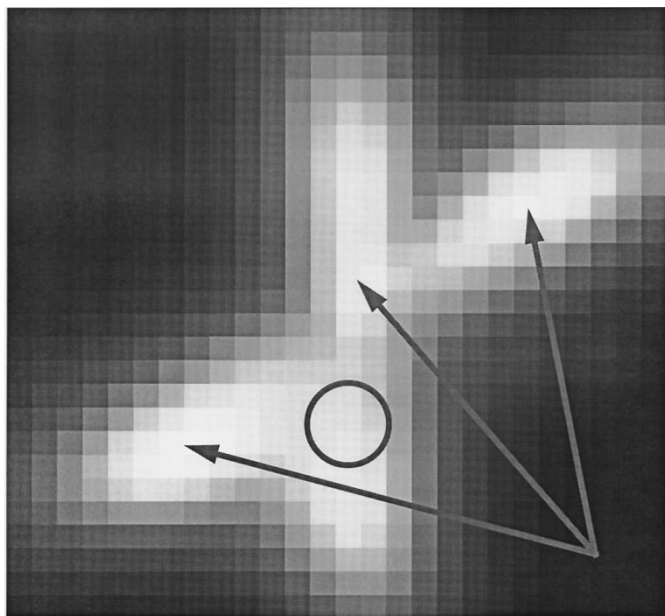


Fig. 4. MUSIC scan of MEG dipolar models, imaging the subspace correlation between model and signal subspace in the plane $z = 7.0$ cm. The arrows indicate the true locations. The noise and partial ambiguities of dipolar models makes discerning each peak difficult, particularly in three dimensions; the circle indicates a source location nearly ambiguous with the three true solutions. The maximum correlation was located in the grid and then used to initiate a directed search for a refined maximum of 99.3% correlation at the correct solution of $[-1.0, -1.0, 7.0]$ cm (rounded to 1 mm).

Note that in Fig. 4, three peaks correspond to the correct dipole locations, and a fourth peak (indicated by the circle) represents an incorrect location. This fourth peak corresponds approximately to a dipole location that would give a local minimum in a least squares search. Since the height of the peak corresponding to this incorrect source location was nearly that of the third true source location, a MUSIC scan that picks out the three largest peaks could mislocate one of the dipoles. Similarly, since we have overspecified the true signal subspace rank, we might erroneously infer that there were four sources. This incorrect location was the cumulative result of the partial correlations of the three correct locations yielding a near ambiguous additional solution. As we will see below, RAP-MUSIC avoided this problem.

The initial location of the first source was taken as the global maximum on the grid in Fig. 4. We refined the estimated location of this first source by searching between the grid points using a Nelder–Meade simplex method to find the source point of maximum correlation. We then projected the signal subspace, and the gain matrices for each grid point, away from the subspace spanned by the array manifold vector for the first source and then ran the second recursion of RAP-MUSIC, i.e., computed the subspace correlation in (10). In Fig. 5, we see the image resulting from computing these subspace correlations for each grid point, and we note that the first source is now suppressed. We again performed a directed search about the maximum on the grid to refine the location of the second source. With the second source located, we again extracted its orientation and formed the two-source array manifold matrix (12). Each grid point and the signal subspace were then projected away from the span of this

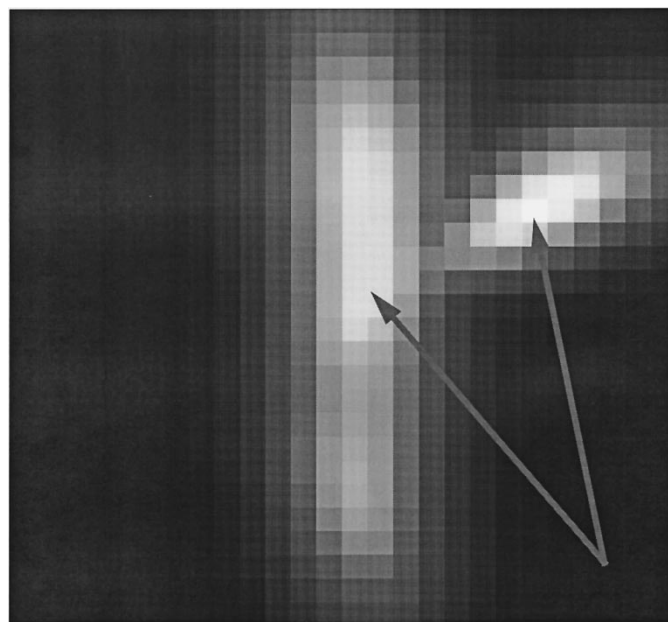


Fig. 5. MUSIC scan of subspace correlation after projecting both the manifold and signal subspace away from the solution of Fig. 4. The MUSIC peak from the first source is suppressed, and we readily performed a directed-search for the maximum of this second correlation: 99.3% at $[1.0, 0.6, 7.0]$. The true solution is 1 mm different at $[1.0, 0.5, 7.0]$. Note the increased suppression of the ambiguous source indicated in Fig. 4.

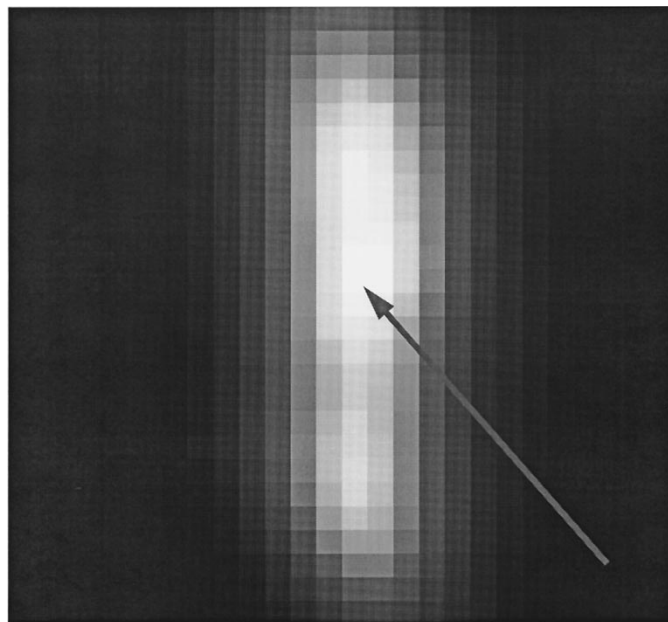


Fig. 6. MUSIC scan of subspace correlation after projecting away the first two solutions. The MUSIC peaks from the first two sources are suppressed, and we readily performed a directed-search for the maximum of this third correlation: 99.2% at $[0, 0.1, 7.0]$. The correct solution is 1 mm away, $[0.0, 0.0, 7.0]$. The search for a fourth solution yielded a principal correlation of only 26.7%, halting the recursion.

matrix and the subspace correlations computed according to (11). The resulting image of the subspace correlations used to find the third source are displayed in Fig. 6. Again, a directed-search algorithm refined the location of the maximum. Repeating the process to look for a fourth source, we found a maximum correlation over the set of grid points of 27%,

indicating that there were no additional identifiable sources present.

This single example is included to demonstrate the potential of RAP MUSIC in higher dimensional source localization problems and to emphasize that the method can cope with overestimation of the dimension of the signal subspace. A more detailed evaluation of the performance of this approach in MEG source localization and extensions to the case of synchronous dipolar sources and nondipolar sources will be presented in a future publication.

VII. CONCLUSIONS

We have presented a novel framework, based on the principal angles between subspaces, in which to view MUSIC and its variations. The MUSIC methods replace the search for multiple sources with procedures for separately identifying each source. For multiple sources, classical MUSIC requires the identification of multiple local maxima in a single metric. Although it is straightforward to identify the first source using the global maximum of this metric, finding subsequent sources requires a peak-picking procedure and can lead to errors, particularly when these sources are weak or strongly correlated with the first source. The other sequential MUSIC forms presented here are measures designed to make localization of the second source more straightforward. Our modifications (R-MUSIC and RAP-MUSIC) are derived from a canonical correlations perspective. Our original R-MUSIC algorithm, which has been derived for MEG research, had error performance comparable to S-MUSIC, but the numerical studies presented here show RAP-MUSIC to yield improved performance over the other forms of MUSIC when the sources are highly correlated; all of the techniques performed well for uncorrelated or slightly correlated cases. Extensions of the RAP-MUSIC approach to many sources and higher dimensionality of the manifold are also more straightforward than the other sequential forms. Finally, the recursive nature of RAP-MUSIC allows the automatic termination of the search for additional sources when the signal subspace rank is overestimated.

ACKNOWLEDGMENT

The authors would like to thank K. Buckley of Villanova University and the anonymous reviewers for their comments on an earlier version of this paper.

REFERENCES

- [1] R. O. Schmidt, "Multiple emitter location and signal parameter estimation," *IEEE Trans. Antennas Propagat.*, vol. AP-34, pp. 276–280, Mar. 1986. Reprint of the original 1979 paper from the *RADC Spectrum Estimation Workshop*.
- [2] ———, "A signal subspace approach to multiple emitter location and spectral estimation," Ph.D. dissertation, Stanford Univ., Stanford, CA, Nov. 1981.
- [3] H. Krim and M. Viberg, "Two decades of signal processing: The parametric approach," *IEEE Signal Processing Mag.*, vol. 13, pp. 67–94, July 1996.
- [4] J. C. Mosher, "Localization from near-source quasi-static electromagnetic fields," Ph.D. dissertation, Univ. Southern Calif., Los Angeles, Mar. 1993 (Los Alamos Tech. Rep. LA-12622-T).
- [5] J. C. Mosher, T. M. Rynne, and P. S. Lewis, "MUSIC for thunderstorm localization," in *Proc. IEEE 27th Asilomar Conf. Signals, Syst., Comput.*, Pacific Grove, CA, Nov. 1993, pp. 986–990.

- [6] M. Hämäläinen, R. Hari, R. J. Ilmoniemi, J. Knuutila, and O. V. Lounasmaa, "Magnetoencephalography—Theory, instrumentation, and applications to noninvasive studies of the working human brain," *Rev. Modern Phys.*, vol. 65, no. 2, pp. 413–497, 1993.
- [7] E. Ferrara and T. Parks, "Direction finding with an array of antennas having diverse polarizations," *IEEE Trans. Antennas Propagat.*, vol. AP-31, pp. 231–236, Mar. 1983.
- [8] J. C. Mosher, P. S. Lewis, and R. M. Leahy, "Multiple dipole modeling and localization from spatio-temporal MEG data," *IEEE Trans. Biomed. Eng.*, vol. 39, pp. 541–557, June 1992.
- [9] G. H. Golub and C. F. Van Loan, *Matrix Computations*, 2nd ed. Baltimore, MD: Johns Hopkins Univ. Press, 1984.
- [10] K. M. Buckley and X. L. Xu, "Spatial-spectrum estimation in a location sector," *IEEE Trans. Acoust., Speech, Signal Processing*, vol. 38, pp. 1842–1852, Nov. 1990.
- [11] J. Vandewalle and B. De Moor, "A variety of applications of singular value decomposition in identification and signal processing," in *SVD and Signal Processing, Algorithms, Applications, and Architectures*, E. F. Deprettere, Ed. Amsterdam, The Netherlands: Elsevier, 1988, pp. 43–91.
- [12] H. Wang and M. Kaveh, "On the performance of signal-subspace processing—Part 1: Narrow-band systems," *IEEE Trans. Acoust., Speech, Signal Processing*, vol. ASSP-34, pp. 1201–1209, Oct. 1986.
- [13] R. Roy and T. Kailath, "ESPRIT—Estimation of signal parameters via rotational invariance techniques," *IEEE Trans. Acoust., Speech, Signal Processing*, vol. 37, pp. 984–995, July 1989.
- [14] S. K. Oh and C. K. Un, "A sequential estimation approach for performance improvement of eigenstructure-based methods in array processing," *IEEE Trans. Signal Processing*, vol. 41, pp. 457–463, Jan. 1993.
- [15] P. Stoica, P. Handel, and A. Nehorai, "Improved sequential MUSIC," *IEEE Trans. Aerosp. Electron. Syst.*, pp. 1230–1239, Oct. 1995.
- [16] J. C. Mosher and R. M. Leahy, "Recursively applied MUSIC: A framework for EEG and MEG source localization," *IEEE Trans. Biomed. Eng.*, vol. 45, pp. 1342–1354, Nov. 1998.
- [17] ———, "Source localization using recursively applied and projected (RAP) MUSIC," in *Proc. Thirty First Annu. Asilomar Conf. Signals, Syst. Comput.*, Pacific Grove, CA, Nov. 2–5, 1997.



John C. Mosher received the B.S. degree in electrical engineering with highest honors from the Georgia Institute of Technology, Atlanta, in 1983. He received the M.S. and Ph.D. degrees in electrical engineering from the Signal and Image Processing Institute, University of Southern California, Los Angeles, in 1985 and 1993, respectively.

From 1979 to 1983, he was also a cooperative education student with Hughes Aircraft Company, Fullerton, CA. From 1983 to 1993, he worked at TRW, Los Angeles, researching signal analysis procedures for electromagnetic pulse effects. In 1993, he accepted a staff position at the Los Alamos National Laboratory, Los Alamos, NM, where he researches the forward and inverse modeling problems of electrophysiological recordings. A member of the Design Technologies Group, his interests also include the general source localization and imaging problems, both in neuroscience work and in other novel applications of sensor technology.



Richard Leahy was born in Surrey, U.K., in 1960. He received the B.Sc. and Ph.D. degrees in electrical engineering from the University of Newcastle upon Tyne, Newcastle upon Tyne, U.K., in 1981 and 1985, respectively.

In 1985, he joined University of Southern California (USC), Los Angeles, where he is currently a Professor in the Department of Electrical Engineering—Systems and Director of the Signal and Image Processing Institute. He holds joint appointments with the Departments of Radiology and Biomedical Engineering at USC. His research interests lie in the application of signal and image processing theory to biomedical inverse problems. His current research involves the reconstruction and analysis of medical images with an emphasis on PET, MEG, and MRI.